Analysis of Evaporation of Cadmium Sulfide for Manufacture of Solar Cells

Vacuum sublimation of cadmium sulfide for manufacture of thin film solar cells was analyzed. The sublimation unit consisted of a two chamber cylindrical source bottle having a rate control orifice and exit nozzle. Coupled heat and mass balance equations were solved using appropriate rate equations for flow in the free molecular-to-viscous transition regime. The model equations predicted that heat transfer has a significant effect on sublimation rate. Experiments were carried out over a range of temperatures with several rate control orifices and exit nozzles. Quantitative agreement between measured rates and those calculated from the model equations was obtained.

R. E. ROCHELEAU, B. N. BARON and T. W. F. RUSSELL

Institute of Energy Conversion
and
Department of Chemical Engineering
University of Delaware
Newark, DE 19711

SCOPE

The economic utilization of solar energy through direct conversion of sunlight to electricity requires development of efficient photovoltaic cells and low cost manufacturing technologies. Thin film solar cells using cadmium sulfide are leading candidates. At the laboratory scale, cells are made by vacuum coating cadmium sulfide on a substrate. The vacuum coating process involves sublimation of cadmium sulfide powder from a heated chamber and condensation onto a cooler substrate. The laboratory process has been sufficiently well developed so that cells having conversion efficiencies over 9% can be made in small quantities.

Design of a commercial scale process and equipment is analogous to chemical reactor design. Ideally, design of the commercial scale unit is based on analysis of laboratory experience, followed by unit operations experimentation. For this paper we have analyzed the laboratory scale sublimation of cadmium sulfide that is used for CdS/Cu_2S solar cells fabrication. The sublimation system consisted of a two compartment cylindrical chamber having a rate control orifice and exit nozzle. Mass and energy balances were derived. The coupled balance equations were solved numerically using appropriate rate equations. The fluid mechanical situation involved flow through orifices and short pipes in the free molecular-to-viscous transition regime. The rate expression was developed for congruent dissociative evaporation of a binary compound in a form such that available thermochemical data could be used to evaluate the properties of the gas.

Experiments were carried out in which the rate of sublimation was measured over a range of wall temperatures for several sets of orifice and exit nozzle dimensions. Predictions based on the model equations were compared to measured rates and the model was verified to a point where design of a unit operations scale system could be carried out.

CONCLUSIONS AND SIGNIFICANCE

Unsteady state mass and energy balances on a charge of solid cadmium sulfide subliming in a nearly closed cylindrical chamber and effusing through a small orifice have been written and numerically solved. The results show that heat transfer from the chamber walls to the subliming surface significantly affects the rate of effusion. The magnitude of this effect depends on the orifice dimensions, geometry of the chamber, and the surface area of the charge. Even with the very large surface area of the charge, the surface temperature can be significantly cooler than the walls. Thus, the common assumption of equal wall and charge temperature is not generally valid. For cadmium sulfide there can be a ten fold error in predicted rate if heat transfer between the wall and charge is ignored.

Using available literature data to estimate material properties (emissivity, density, etc.), the model agrees with experiment over a wide range of orifice areas and chamber temperatures. The verified model equations provided the basis for design of a unit operations scale system which will be described in a subsequent publication.

This work represents the initial stage in the application of the logic and procedures of reactor design to solar cell manufacture.

INTRODUCTION

Thin-film CdS/Cu_2S solar cells with conversion efficiencies over 9% have been made in the laboratory utilizing thermal evaporation of CdS in a process described by Hall and Meakin (1979). Since large areas of solar cells must be deployed in order to generate significant amounts of energy, a low-cost commercial manufacturing process must be developed. An essential part of this process is a unit which uniformly deposits material over large areas.

Laboratory scale deposition of CdS by thermal evaporation takes place in a system similar to that in Figure 1. The rate of evaporation

Correspondence concerning this paper should be addressed to T. W. F. Russell.
0001-1541-82-5769-0656-$2.00.

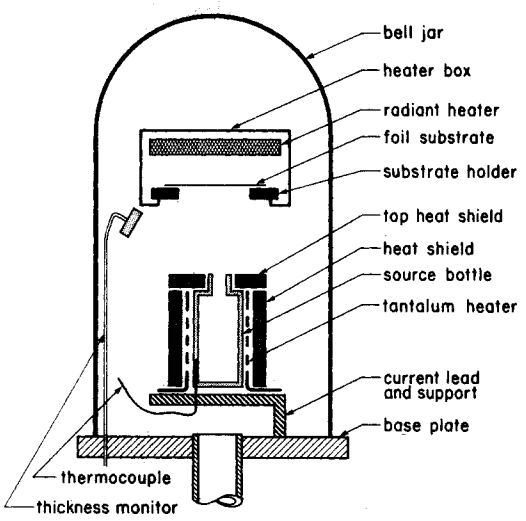

Figure 1. Laboratory scale CdS deposition system.

is determined by the surface temperature of the evaporating CdS which depends on bottle design, geometry, surface area of the CdS, and the heater design.

CdS powder is placed in the graphite source bottle. Current is passed through the tantalum resistance heater, heating the crucible. The effusion rate is measured by the quartz crystal thickness monitor. If the material is depleted in such a fashion as to reduce its surface area, the power to the heater must be increased to maintain rate. Sublimed CdS condenses on the substrate which is controlled at a temperature of 450 to 525K and is 0.08 to 0.20 m away from the source. In the laboratory operation described by Hall and Meakin (1979), CdS is deposited at rates of 80 to 160 kg/m^2-s on zinc plated copper foil. In this batch operation, less than ten percent of the sublimed CdS condenses on the substrate.

This paper presents a model for the rate of sublimation and effusion of a solid material from a cylindrical source. The model is compared to experimental results obtained with CdS.

MODEL EQUATIONS

Physical Situation

The system to be modeled is shown in Figure 2a. Powdered CdS is packed into the cylindrical graphite bottle which has a thermocouple well in the wall for accurate temperature measurement. The cap with a large diameter nozzle is separated from the powder by a removable orifice plate. Upon heating with the tantalum resistance heater, CdS dissociates and sublimes. Material flows from the chamber containing the solid CdS through the rate controlling orifice into the second chamber, then through the outer nozzle into a high vacuum region, $P < 0.01$ Pa. No condensation occurs in the nozzles or in the chamber between the rate orifice and removable cap. The packed CdS retains the cylindrical shape, shrinking both in height and diameter (Figure 2b) as the material is depleted.

Mass and Energy Balance

The mass balance for a control volume consisting of the material in the bottle when there is negligible material in the vapor phase is

$$\frac{\partial \rho V}{\partial t} = -\rho_g q \tag{1}$$

The energy balance around material in the bottle for an isothermal wall, assuming an isothermal charge with heat transfer solely by radiation is

$$\rho V C_p \frac{\partial T_1}{\partial t} = -\rho_g q \Delta H_R + F_v F_\epsilon \sigma (T_2^4 - T_1^4) A_s \tag{2}$$

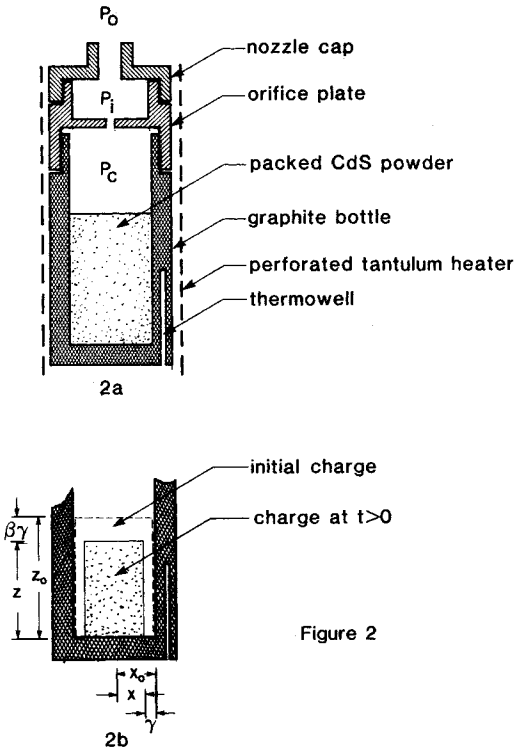

Figure 2

Figure 2. Source for CdS evaporation. 2a. Bottle and cylindrical charge. 2b. Coordinate system for model equations.

The temperature of the chamber wall can change with time. This temperature can be calculated from an additional energy balance around the source bottle and heater. In practice, the wall temperature T_2, is measured. Equations 1 and 2 can then be solved numerically given the initial charge dimensions and appropriate constitutive expressions for the mass flux.

The differential mass and energy balances can be rewritten in terms of the initial charge dimensions; the change in the radius of the charge, γ; and the change in the height of the charge, $\beta\gamma$. A convenient form of $\partial\gamma/\partial t$ is obtained when β is constant. Using this approximation and the coordinate system in Figure 2b, the mass and energy balances reduce to:

$$\frac{\partial \gamma}{\partial t} = \frac{1}{\pi \rho}\left(\rho_g q + V \frac{d\rho}{dt}\right)[\beta(x_0 - \gamma)^2 + 2(x_0 - \gamma)(z_0 - \beta\gamma)]^{-1} \tag{3}$$

$$\frac{\partial T_1}{\partial t} = F_v F_\epsilon \sigma \frac{(T_2^4 - T_1^4)A_s + \rho_g q(-\Delta H_R)}{\rho V C_p} \tag{4}$$

Solution of Eqs. 3 and 4 requires the input of materials and geometry dependent parameters such as the view factor, effective emissivity, heat of vaporization and heat capacity; and an equation for the mass flow rate, $\rho_g q$. Equations for the effusion of gases through small orifices and tubes are developed in the next section. The modifications and limitations for multicomponent gases are also presented. Finally, the model equations are solved for the particular case of Cd and S_2 vapor resulting from the sublimation of cadmium sulfide.

Constitutive Flow Equations

In a system such as in Figure 2 the net rate of phase change is determined from the rate of effusion through the orifices. The effusion rate depends on the vapor pressure of species inside the bottle, the vapor composition, and geometry of the orifices.

At low pressure, it is common to describe flow on the basis of the ratio of the mean-free-path of molecules in the chamber to the orifice radius, or Knudsen number. Three regimes of flow are commonly defined: free molecular; transitional; and viscous. When the Knudsen number is less than 0.01, the flow is considered viscous;

TABLE 1. CONSTITUTIVE FLOW EQUATIONS

Flow Regime	Orifice	Pipe
Free Molecular $\lambda_m/\Gamma > 1$)	$r = (Mg_c/2\pi RT)^{1/2}(P_1 - P_2)$	$r = \frac{g_c\Gamma^2 M}{16\mu LRT}(P_1^2 - P_2^2)\left(4\left(\frac{2}{f} - 1\right)\frac{\lambda_m}{\Gamma}\right)$
Viscous ($\lambda_m/\Gamma < 0.01$)	$r = C_o Y\,[2\rho g_c(P_1 - P_2)]^{1/2}$	$r = \frac{g_c\Gamma^2 M}{16\mu LRT}(P_1^2 - P_2^2)$

greater than 1.0, free molecular. The flows described in this paper fall within the categories of free molecular flow and the transitional regime between free molecular and viscous flow. The important equations for viscous and free molecular flow through pipes and orifices are summarized in Table 1.

Discussions of free molecular flow are presented by Dushman (1962) and by Brown et al. (1946). The mean free path, λ_m, from kinetic theory is

$$\lambda_m = (\pi RT/2g_cM)^{1/2}\mu/p_m \tag{5}$$

Using this relationship, the equations for free molecular flow in orifices and pipes presented in Table 1 can be written as

$$r_f = K(Mg_c/2\pi RT)^{1/2}(p_1 - p_2) \tag{6}$$

where K is unity for an ideal orifice and equals $\pi/2(2/f - 1)\Gamma/L$ for a long pipe. For aspects ratios, L/Γ, between these extremes, Kennard's (1938) analysis provides a useful expression for K:

$$K = (1 + 0.5\,L/\Gamma)^{-1} \text{ for } L/\Gamma \le 1.5$$

and

$$K = (1 + 0.4)\,L/\Gamma)/(1 + 0.95\,L/\Gamma + 0.15(L/\Gamma)^2) \quad \text{for } L/\Gamma > 1.5 \tag{7}$$

The physical situation addressed in this paper corresponds to aspect ratios, L/Γ, between 1 and 4; intermediate between true orifices where only entrance effects are important and pipe flow where entrance effects are negligible. Thus, Eq. 6 with K ranging from 0.67 to 0.36 is applicable at the lower rates (when $\lambda_m/\Gamma >$ 1). At the higher rates, the flows are within the transition regime with the Knudsen number between 0.01 and 1.0. A suitable calculation procedure in this regime is the semi-empirical procedure described by Brown et al. (1946). The total pressure drop is obtained by adding the pressure drops calculated for a contraction at the entrance using Eq. 6, with $K = 1$, and the drop through the tube using a modified form of Poiseuille's equation. The mass flux in the transition reigme is

$$r_t = C(Mg_c/2\pi RT)^{1/2}(p_1 - p')$$

or

$$r_t = \frac{g_c\Gamma^2}{16\mu L}(p'^2 - p_2^2)\left(1 + 4.0\left(\frac{2}{f} - 1\right)\frac{\lambda_m}{\Gamma}\right)(M/RT) \tag{8}$$

The pressure at the tube entrance after entrance losses, p', is calculated by iteration from Eqs. 8 for a fixed value of C.

For multicomponent systems, the parameters used in the constitutive flow equations (Eq. 6 or 8) such as mean free path, molecular weight, and viscosity and pressure must be those of the mixture. The estimation of these values for vapors resulting from the evaporation and effusion of a dissociating compound are described below.

Composition of Vapor

Many compounds, including cadmium sulfide, dissociate upon evaporation according to:

$$(AB)_s \rightleftarrows A_g + 1/n(B_n)_g \tag{9}$$

For systems such as the effusion source in Figure 2, the characterizing physical properties of the gas will vary as the dynamics of the flow change.

For a two component gas effusing under free molecular flow conditions, the mass flux of each species is described by equation 6 with the appropriate component data. Rewriting these for molar flux one obtains:

$$\tilde{r}_A = K(g_c/2\pi RT_1M_A)^{1/2}P_A \tag{10}$$

$$\tilde{r}_{B_n} = K(g_c/2\pi RT_1M_{B_n})^{1/2}P_{B_n} \tag{11}$$

At steady state, congruent evaporation assures that one mole of species A and $1/n$ moles of species B_n effuse for each mole of solid AB that sublimes. The ratio of partial pressures from Eqs. 10 and 11 with this constraint is

$$\frac{P_A}{P_{B_n}} = n\left(\frac{M_A}{M_{B_n}}\right)^{1/2} \tag{12}$$

Expressing the total mass flux of both A and B_n, (r_{AB}), in terms of the component molar flux (Eq. 10 or 11) and the molecular weight of the condensed phase (M_{AB}); and solving for the component pressures gives:

$$P_A = r_{AB}(M_{AB}K)^{-1}(2\pi RT_1M_A/g_c)^{1/2} \tag{13}$$

$$P_{Bn} = r_{AB}(M_{AB}K)^{-1}(2\pi RT_1M_{B_n}/g_c)^{1/2} \tag{14}$$

Since the total pressure is the sum of partial pressures, Eqs. 13 and 14 can be combined and solved for the total mass flux r_{AB}. Since p_1 is the upstream pressure and p_2 the downstream pressure, the total mass flux through the orifice is described by

$$r_{AB} = K(g_c/2\pi RT_1)^{1/2}\frac{nM_{AB}}{M_{B_n}{}^{1/2} + nM_A{}^{1/2}}(p_1 - p_2) \tag{15}$$

Equation 15 is a restatement of equation 6 for dissociative evaporation and free molecular flow where the effective molecular weight of the mixture is

$$M = \left[\frac{nM_{AB}}{M_{B_n}{}^{1/2} + nM_A{}^{1/2}}\right]^2 \tag{16}$$

Solution of the model equations requires an expression for the vapor pressure of evaporant in the chamber. The equilibrium constant for the reaction described by Eq. 9 assuming ideal gas behavior is

$$K_p(T_1) = P_AP_{B_n}{}^{1/n} \tag{17}$$

The equilibrium constant and vapor composition (Eq. 12) are sufficient to calculate the vapor pressure under free molecular flow conditions:

$$P_e = K_p{}^{n/(n+1)}[n^{1/(n+1)}(M_A/M_{B_n})^{1/(2n+2)} + n^{-\int n/(n+1)}(M_A/M_{B_n})^{-n/(2n+2)}] \tag{18}$$

In the case of effusion of a congruently dissociating compound with flows in the viscous regime the steady state vapor composition will result directly from the dissociation reaction so that

$$P_A = nP_{B_n} \tag{19}$$

The vapor pressure in the viscous regime is

$$P_e = K_p{}^{n/(n+1)}[(1 + n)n^{-n/(1+n)}] \tag{20}$$

The viscosity and an effective molecular weight are also needed for the viscous flow equation (Table 1).

The viscosity of the gas mixture can be calculated from the component data using the method of Wilke (1950). The component viscosities are calculated using Chapman-Enskog theory (Reid et al., 1977) with molecular interaction parameters calculated from the phase transition temperatures (melting, boiling or critical point), Bird et al. (1960). The effective molecular weight for the stoichiometric vapor associated with viscous flow (Eq. 19) is described by Eq. 16.

The composition of the gas for flows in the transition regime will be between the free molecular and viscous regime values. Evaluation of the gas properties at both extremes for Eq. 8 provides useful limits for design calculations.

SOLUTION OF MODEL EQUATIONS

The rate of effusion of CdS subliming from a solid cylinder through a series of orifices (Figure 2) can be calculated using the non-steady state mass and energy balances, Eqs. 3 and 4, with the appropriate constitutive flow equation. Material dependent properties are available from the literature. The remaining model parameters are determined by experiment. The entrance loss coefficient, C, defined by Brown et al. is an adjustable parameter used to fit the data.

Physical Properties and Model Parameters for CdS

Below 1,673 K and 1.01×10^5 Pa pressure the phase change of CdS occurs as a solid-vapor transition. Studies by Berkowitz and Marquart (1963) and Jeunehomme (1962) using mass spectrometric techniques show that the sublimation of CdS proceeds by the overall reaction:

$$(CdS)_s \rightleftarrows Cd_g + (S_2)_g^{1/2} \tag{21}$$

The vapor pressures predicted by Eqs. 18 and 20 for the dissociation of cadmium sulfide differ by less than one percent. The equilibrium pressure can therefore be described by a single equation for any of the flow regimes discussed. Based on data reported by Goldfinger and Jeunehomme (1963), Pogerelyi (1948), Spandau and Klanberg (1959), and Veselovskii (1942), the equilibrium vapor pressure is

$$P_e = 1.572 \times 10^{12} \exp\left[-2.633 \times 10^4/T\right] \tag{22}$$

The heat of vaporization for this dissociation reaction is 3.28×10^8 J/kg-mol.

The composition of the vapor in the nearly closed chamber will vary from 72.6 mol % cadmium in the free molecular flow regime (Eq. 12) to 66.7 mol % cadmium under viscous flow conditions (Eq. 19). Viscosities were calculated at both composition extremes for rate calculations in the transition regime. The characteristic parameters of the component species were evaluated from boiling point correlations.

Somorjai (1962) and Somorjai and Jepson (1963, 1964) have studied the mechanism of CdS sublimation for single crystals. Their analysis using Langmuir kinetics showed that surface dissociation is the rate limiting step with evaporation from the surface being up to six times slower than predicted from the equilibrium pressures. If the surface area of the condensed phase is not sufficiently large relative to the orifice area, the vapor pressure in the evaporation chamber (P_c, Figure 2) will be lower than the equilibrium value (P_e). A procedure to estimate the actual evaporation chamber pressure for the geometries used in these experiments is described below.

Kern (1950) shows that the effective emissivity and view factor ($F_v F_\epsilon$) for concentric cylindrical surfaces is

$$F_v F_\epsilon = \left(\frac{1}{\epsilon_{CdS}} + \frac{A_s}{A_{ext}}\left(\frac{1}{\epsilon_{gr}} - 1\right)\right)^{-1} \tag{23}$$

The emissivity of graphite used was 0.70, based on data presented by Gebhart (1971) and by Rohsenow and Hartnet (1973). The hemispherical emissivity of CdS was calculated at 373 and 473 K from the spectral emissivity data of Stierwalt (1962). The calculated value of 0.45 at 473 K and extropolated value of 0.15 at 1,273 K were used to set upper and lower limits in the model. The heat capacity of solid CdS from Russell (1912) is

$$C_p = 5.40 \times 10^4 + 3.76\,T \tag{24}$$

The model parameters β and $d\rho/dt$ were evaluated from the experimental data. This analysis is discussed in the results.

Solution Method

Model Eqs. 3 and 4 were solved numerically using an available computer program for simultaneous first order differential equations. In addition to the physical properties and model parameters previously described, the wall temperature of the chamber and initial charge dimensions and mass were provided as input. At each time increment the charge temperature, T_1, and the remaining charge mass and dimensions were computed.

The calculation of the rate of effusion, $\rho_g q$, at each increment required iterations to calculate the pressure (P_i, Figure 2) in the intermediate chamber and the pressure in the evaporation chamber (P_c, Figure 2). The rate of effusion at each time increment was first calculated assuming the vapor in the inner chamber is in equilibrium with the condensed phase at the solid temperature, T_1. The pressure in the intermediate chamber (P_i) was then determined iteratively by equating the effusion rate through the inner and outer orifices. The effusion rate through each orifice was calculated using the free molecular rate equation for binary gas mixtures (Eq. 15) when the Knudsen number at the mean pressure in the orifice was greater than 1.0; and with Eq. 8 and the multicomponent parameters when the Knudsen number was less than 1.0.

After convergence of the two orifice rates, a numberical iteration to estimate the pressure in the evaporation chamber (P_c) was carried out. In this procedure, a new evaporation chamber pressure ($P_c \neq P_e$) was estimated by equating the net effusion rate at pressure P_c to the net rate of evaporation from the surface of the condensed phase. The rate from the surface was based on a driving force equal to ($P_e - P_c$) and a kinetic limitation which reduced this rate to 16% (Somorjai, 1962) of the unlimited rate. Details of the computational procedure are discussed by Rocheleau (1981).

Values of the charge temperature, net rate of evaporation and total mass loss of CdS were calculated at one minute intervals for comparison with the experimental data.

EXPERIMENTAL

Thirty cadmium sulfide evaporation runs were made to verify the model equations and constitutive rate expressions. The CdS was evaporated from the cylindrical graphite source (0.025 m dia. × 0.070 m), Figure 2, placed in a Varian NRC 3118 vacuum coater system. The graphite wall temperature was measured with an Inconel sheathed chromel-alumel thermocouple inserted in the thermowell to a height in the middle of the charge. Power to the tantalum heater was controlled using a Eurotherm SCR unit through a step-down filament transformer. A water cooled calibrated quartz crystal thickness monitor (Kronos Model QM311 by Veeco Inc.) was used to measure the evaporated mass versus time. The value of thickness displayed by the monitor is directly proportional to the total mass of material condensed on the quartz crystal surface. The mass accumulated on the quartz crystal is directly proportional to the total mass which has effused from the source, the proportionality constant being the total mass loss divided by the final monitor reading. The experimental rate of evaporation is the slope of this mass loss-time curve.

Twenty-seven runs began with 0.035 kg of electronic grade CdS powder (General Electric Co., Cleveland, OH) packed to an approximate density of 1,800 kg/m^3 in the bottom chamber. The remaining three runs began with approximately half of this charge. With bell jar pressure in the range 1.33×10^{-4} to 1.33×10^{-3} Pa, the source was heated to between 675 and 975 K for 600 to 1,800 seconds to outgas the CdS and vacuum system. After setting the controller to the selected temperature for the run; wall temperature, ambient chamber pressure, and mass on the quartz crystal were recorded at one minute intervals. Heat-up and cool-down times were minimized to allow maximum time at 'design' temperature. After cooling, the source and CdS were weighed to determine the total weight loss. The

dimensions of the remaining CdS were recorded for final density determination.

The parameters controlling the rate of evaporation were varied to give over a 50 fold change in rate. The range of rates corresponded to those anticipated for pilot plant operation. The rate orifice area varied from 2 $\times 10^{-6}$ m^2 to 13 $\times 10^{-6}$ m^2 while the wall temperature varied from 1,113 to 1,333 K. The exit nozzle area varied from 15 $\times 10^{-6}$ m^2 to 26 $\times 10^{-6}$ m^2.

RESULTS

The model equations were solved for the evaporation conditions found in each of the 30 experiments.

The CdS powder in the source sinters during evaporation resulting in a change in density, and a possible difference in the rate of change of height and radius of the charge ($\beta \neq 1$). The dimensions of the charge were measured before and after evaporation to obtain an empirical expression for the density change ($d\rho/dt$) and the value of β.

Final charge densities were accurately predicted when the density was assumed to increase linearly at 0.17 kg/m^3/s during the time the charge was above 973 K. The calculated mass loss assuming either no density change or an instantaneous change before evaporation differed by less than five percent from the linear model.

The data used to estimate the rate of change of density were used to estimate β, the ratio of the change in charge height to radius during the run. The average value of β was 1.9 with a standard deviation of 0.60. The model was quite insensitive to the value of β. A 50% variation in β changes the calculated mass loss by less than one percent.

Changing the vapor composition from 72.4 mol % to 66.7 mol % cadmium resulted in less than a two percent change in the calculated rate of effusion in the transition regime. This change is less than that due to a one degree change in charge temperature. Accordingly, a vapor composition of 72.4 mol % cadmium was used for the analysis of data without regard to flow regime.

It was found that the flow through both orifices occurred within the defined transition regime except at the very low startup and cooldown temperatures. The entrance loss coefficient C (Eq. 8) was set equal to 20. A series of calculations showed that mass loss decreases by less than 8%, if C equals 10; mass loss increases by less than 3.5%, if C equals 30. When C equals 20, 5.0 to 25.0% of the total pressure drop is attributed to contraction at the entrance and the rest to the orifice walls.

The ratio of charge surface area to orifice area was large enough in the experiments to maintain the chamber pressure within 3% of the equilibrium value.

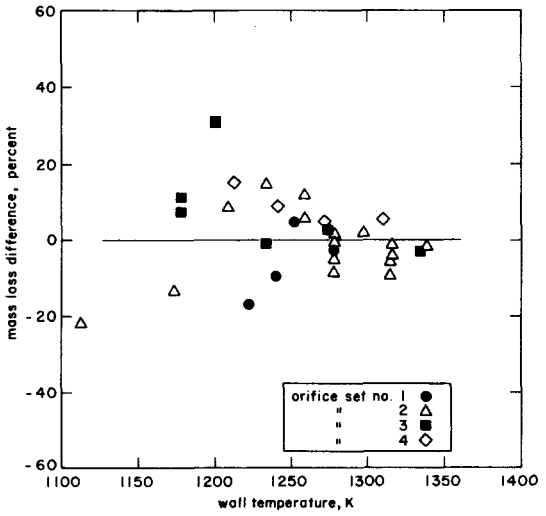

Figure 3. Percent difference between calculated and measured total CdS mass loss as function of steady state wall temperature.

The CdS emissivity was taken to be 0.25. A 20% change in the emissivity changes the calculated rates by 6 to 15%, the greater changes occurring with larger orifices at high temperature.

Output from the solution of the model equations, at one minute intervals, was: temperature of the CdS charge; remaining weight of CdS; charge surface area; and calculated effusion rate.

Total mass losses, predicted and measured, can be directly compared since the calculated losses included the initial heatup and terminal cooldown stages of each run. The percentage differences between calculated and measured weight losses as a function of specified wall temperature are shown in Figure 3. The large (30%) difference for run number 3039, may be of spurious origin since the mass loss for this run is inconsistent with data from other runs at higher and lower temperatures with the same 0.206

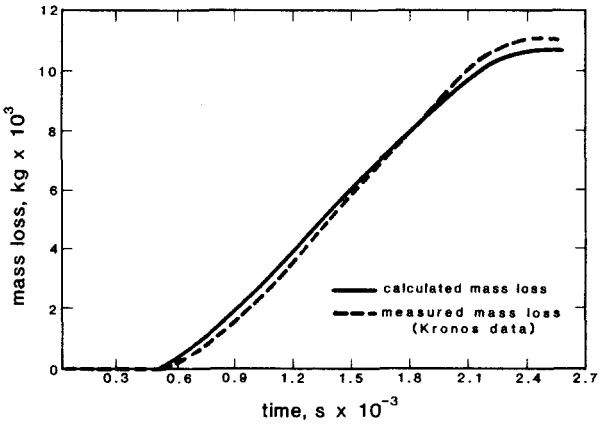

Figure 4. Measured mass loss vs. time: run number, 3007; orifice set, No. 2; wall temperature = 1,277 K.

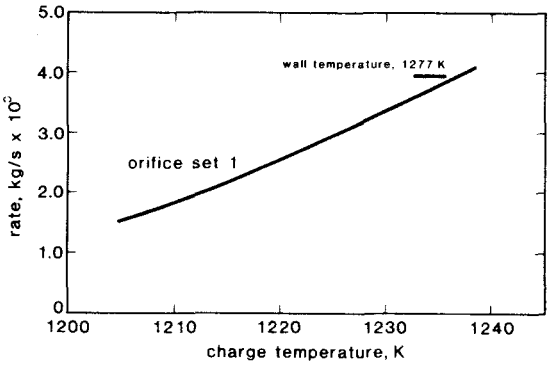

Figure 5. CdS effusion rate vs. charge temperature for orifice set No. 1 (rate orifice 2.03 $\times 10^{-6}$m^2 by 2.06 $\times 10^{-3}$m long, exit nozzle 15.13 $\times 10^{-6}$m^2 by 0.013m long): solid line calculated from model; horizontal bars from mass-time data; wall temperature indicated.

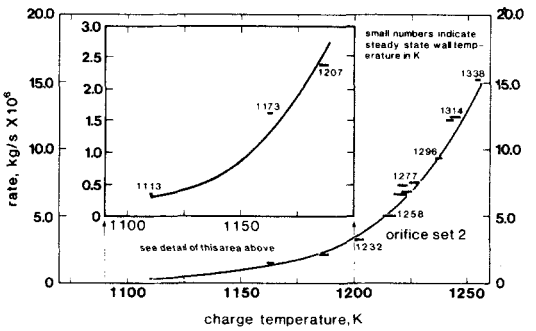

Figure 6. CdS effusion rate vs. charge temperature for orifice set No. 2 (rate orifice 3.33 $\times 10^{-6}$m^2 by 2.06 $\times 10^{-3}$m long, exit nozzle 26.32 $\times 10^{-6}$m^2 by 0.013m long): solid line calculated from model; horizontal bars from mass-time data; wall temperature indicated.

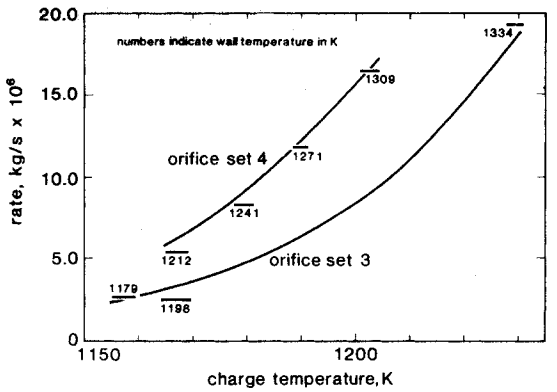

Figure 7. CdS effusion rate vs. charge temperature for orifice set No. 3 (rate orifice 6.47 × 10^{-6}m² by 2.06 × 10^{-3}m long, exit nozzle 26.32 × 10^{-6}m² by 0.013m long) and Orifice Set No. 4 (rate orifice 12.88 × 10^{-6}m² by 2.06 × 10^{-3}m long, exit nozzle 26.32 × 10^{-6}m² by 0.013m long): solid line calculated from model; horizontal bars from mass-time data; experimental wall temperatures indicated.

m diameter rate orifice. The calculated mass loss for 22 of the 29 remaining experiments deviates from the actual mass loss by less than 10%. The seven experiments with larger deviations were carried out at the lower temperatures for each orifice set and these calculated losses varied randomly about the measured value.

The coupled heat and mass balance equations show that the wall temperature and the temperature of the evaporating charge can be quite different. The difference between the charge and wall temperatures increases as the rate increases for a fixed orifice. Failure to properly model the heat transfer leads to serious error at the higher rates. If, for example, the charge temperature is erroneously assumed to equal the measured wall temperature, the calculated rates would be over 100% greater than measured in 24 of the 29 runs with some in error by greater than a factor of ten.

Figure 4 illustrates typical mass versus time behavior, showing both calculated and measured mass losses. Experimental evaporation rate was determined by averaging the slopes of the mass-time data taken in the portion of the curve which corresponds to the steady state constant wall temperature segment of the run, i.e., the linear ascending part of Figure 4. The results are plotted in Figures 5, 6 and 7. The solid curves show rate versus charge temperature calculated from the model for the designated orifice set. The bars are measured rates versus the calculated charge temperature. The length of each bar corresponds to variation in calculated charge temperature at the constant wall temperature. This variation is due to changes in the charge dimensions and density as the charge evaporates.

NOTATION

A_s = surface area of packed CdS
A_{ext} = surface area of surrounding cylinder
C = correction factor for short pipe entrance losses
C_o = orifice coefficient, Bernoulli equation
C_p = heat capacity of CdS, J/kg-mol·K
F_ϵ = effective emissivity
F_v = view factor
K = correction factor for non-ideal orifice
K_p = equilibrium constant for dissociative evaporation
L = pipe or orifice length
M_i = molecular weight, species i
P_j = partial pressure, species j
P_e = equilibrium vapor pressure
P_c = vapor pressure in evaporation chamber
P_i = vapor pressure in intermediate chamber
P_o = ambient pressure in vacuum chamber
R = ideal gas constant
T_1 = temperature of packed CdS
T_2 = temperature of bottle wall
V = volume of packed CdS powder
f = fraction of gas molecules diffusely reflected from wall ($f = 0.9$)
g_c = pressure conversion factor
n = stoichiometric coefficient
p_1 = pressure upstream of orifice or pipe
p_2 = pressure downstream of orifice or pipe
p' = pressure at tube entrance after contraction
p_m = mean pressure
$q.$ = volumetric flow rate of exit stream
r_f = mass flux through orifice or pipe, free molecular flow
r_t = mass flux through orifice or pipe, transition regime
r_{AB} = total mass flux of AB through orifice or pipe
$\tilde{r}_i$ = molar flux of species i
t = time
x_o = initial charge radius
z_o = initial charge height
ϵ_{CdS} = emissivity of CdS
ϵ_{gr} = emissivity of graphite
β = ratio of change in charge height to change in charge radius
γ = change in charge radius
λ_m = mean free path
ρ = bulk density of packed CdS powder
ρ_g = mass density of gas phase
σ = Stefan-Boltzman constant
Γ = pipe or orifice radius
μ = viscosity of gas at mean pressure
ΔH_R = latent heat of vaporization

LITERATURE CITED

Berkowitz, J., and Marquart, "Dissociation Energies of Some Metal Sulfides," *J. Chem. Phys.*, **39**, 283 (1963).

Bird, R. B., W. E. Stewart, and E. N. Lightfoot, *Transport Phenomena*, Wiley, NY, p. 19 (1966).

Brown, G. P., A. D. Nardo, G. K. Cheng, and T. K. Sherwood, The Flow of Gases in Pipes at Low Pressures," *J. of Appl. Phys*, **17**, 802 (1946).

Dushman, S., *Scientific Foundations of Vacuum Technique*, Wiley, New York, p. 84 (1962).

Gebhart, B., *Heat Transfer*, 2nd ed., McGraw-Hill, New York, p. 126 (1971).

Goldfinger, P., and M. Jeunehomme, "Mass Spectrometric and Knudsen Cell Vaporization Studies of Group 2B-6B Compounds," *Trans. Faraday Society*, **59**, 2851 (1963).

Hall, R. B., and J. D. Meakin, "Design and Fabrication of High Efficiency Thin Film CdS/Cu_2S Solar Cells," *Thin Solid Films*, **63**, 203–211 (1979).

Jeunehomme, M., Ph.D. Thesis, Universite Libre de Bruxelles (1962), cited by G. A. Somorjai and D. W. Jepsen, *J. of Chem. Phys.*, **41** (5), 1389 (1964).

Kennard, E. H., *Kinetic Theory of Gases*, McGraw-Hill Book Co., New York, p. 306 (1938).

Kern, E., *Process Heat Transfer*, 1st ed., McGraw-Hill Book Co., New York (1950).

Pogorelyi, A. D., *J. Phys. Chem.*, USSR, **22**, 731, cited by Goldfinger and Jeunehomme (1948).

Reid, R. C., et al., *The Properties of Liquids and Gases*, 3rd ed., McGraw-Hill, New York p. 394 (1977).

Rocheleau, R. E., Ph.D. Thesis, "Design Procedures for a Commercial Scale Thermal Evaporation System to Deposit CdS for Solar Cell Manufacture," University of Delaware (1981).

Rohsenow, W. M., and J. P. Hartnett, eds., *Handbook of Heat Transfer*, McGraw-Hill Co., New York (1973). Chapter 15: *Radiation, Relations and Properties*, by E. R. G. Eckert.

Russell, *Physik*, Z., **13**, 59 (1912), cited by P. Goldfinger and M. Jeunehomme.

Somorjai, G. A., "The Evaporation Rate of CdS and CdSe," *Proc. Intern. Symp. Evaporation and Condensation of Solids*, Dayton, OH (1962).

Somorjai, G. A., and D. W. Jepsen, "Evaporation Mechanism and Vapor Composition," *J. of Chemical Physics*, **39**, (7), 1665 (1963).

Somorjai, G. A., and D. W. Jepsen, "Evaporation Mechanism of CdS Single Crystals: I. Surface Concentration and Temperature Dependence of the Evaporation Rate," *J. of Chem. Physics*, **41** (5), 1389 (1964).

Spandau, H., and F. Klanberg, *Z. Anorg. Chem.*, **295**, 309 (1959), cited by P. Goldfinger and M. Jeunehomme.
Stierwalt, D. L., *Navy Ordnance Lab Report 667*, Corona, CA (1966), cited by W. L. Wolfe, *Handbook of Optics*. Chapter 7, W. G. Driscoll and W. Vaughan, eds., McGraw-Hill, New York (1978).
Veselovskii, B. K., *J. of Appl. Chem.*, USSR, **15**, 422 (1942), cited by P. Goldfinger and M. Juenehomme.
Wilke, C. R., "Viscosity Equation for Gas Mixtures," *J. Chem. Phys.*, **18**, 517 (1950).

Manuscript received January 26, 1981; revision received August 20, and accepted August 31, 1981.

Batch Extraction with Liquid Surfactant Membranes: A Diffusion Controlled Model

A model of diffusion controlled mass transfer in liquid surfactant membranes is developed for uniform emulsion globules having no internal circulation. The solute is assumed to react instantaneously and irreversibly with the internal reagent at a reaction surface which advances into the globule as the reagent is consumed. A perturbation solution to the resulting non-linear equations is presented. In general, the zero-order, or pseudo-steady state solution alone often gives an adequate representation of the process. Experimental data on the batch extraction of phenol from waste water are in good agreement with the model predictions.

W. S. HO
Exxon Research and Engineering Co.
Linden, NJ 07036

T. A. HATTON and E. N. LIGHTFOOT
Department of Chemical Engineering
University of Wisconsin
Madison, WI 53706

and N. N. LI
UOP Inc.
Des Plaines, IL 60016

SCOPE

Mathematical models currently available for predicting the mass transfer performance of liquid-surfactant membrane systems are of limited utility, both because they rely on parameters which cannot be estimated independently of the extraction runs themselves, and because the data obtained from batch experiments generally do not extrapolate to continuous flow situations. The reason is that these models do not adequately reflect the actual mass transfer processes occurring within the LM globules, and it is apparent that a more detailed mathematical modelling approach must be adopted if a meaningful interpretation of experimental extraction data is to be made.

In this work, a model is formulated for the calculation of solute extraction rates in the presence of a diffusion-controlled reaction by uniform emulsion globules dispersed in a well-mixed fluid, and a regular perturbation solution to the model equations is developed. The model is tested experimentally using the extraction of phenol from water by aqueous caustic solutions as the test system.

CONCLUSIONS AND SIGNIFICANCE

The development reported here is the first to provide reasonably accurate predictions, without the use of adjustable parameters, of solute extraction rates in batch liquid membrane systems. The only information required, in addition to pertinent equilibrium and transport properties, is the Sauter mean diameter of the suspended globules. This model thus represents a significant improvement over existing design procedures, both for liquid membranes and analogous processes such as extraction by reactive solvents and heat transfer in the presence of phase changes. Examples of current interest include hydrometallurgy, and the removal of trace contaminants from waste streams.

INTRODUCTION

Since their discovery just over a decade ago (Li, 1968), liquid surfactant membranes have demonstrated considerable potential as effective tools for an increasingly wide variety of separations (Maugh, 1976). These include: 1. the fractionation of hydrocarbons (Li, 1971a, 1971b; Shah and Owens, 1972; Cahn and Li, 1976a, 1976b; Alessi et al., 1980; Halwachs et al., 1980); 2. the recovery and enrichment of heavy metal ions (Schiffer et al., 1974; Hochhauser and Cussler, 1975; Martin and Davies, 1976/1977; Kondo et al., 1979; Völkel et al., 1980; Strzelbicki and Charewicz, 1980;

Correspondence concerning this paper should be addressed to T. A. Hatton, Dept., Chem., Engrg., MIT, Cambridge, MA 02139.
0001-1541-82-6097-0662-$2.00.